

PROJEKT TITLE: Weather in a Box - Autonomous self-powered energy harvesting interface and power management system for sensor applications and wireless data transmission

TEAM LEADER: Maximilian Marx, maxmarx@web.de

TEAM MEMBERS: Florian Kromer, Daniel Schillinger

ADVISING PROFESSOR: Prof. Dr.-Ing. Yiannos Manoli, ymanoli@imtek.de

UNIVERSITY: Albert Ludwigs Universität Freiburg, Germany

DATE: 14.7.2011

TI PARTS USED IN PROJECT:

1x MSP430F2234: <http://focus.ti.com/docs/prod/folders/print/msp430f2234.html>

2x TLV3491: <http://focus.ti.com/docs/prod/folders/print/tlv3491.html>

1x TPS3106E16: <http://focus.ti.com/docs/prod/folders/print/tps3106e16.html>

3x SN74AUP1T97: <http://focus.ti.com/docs/prod/folders/print/sn74aup1t97.html>

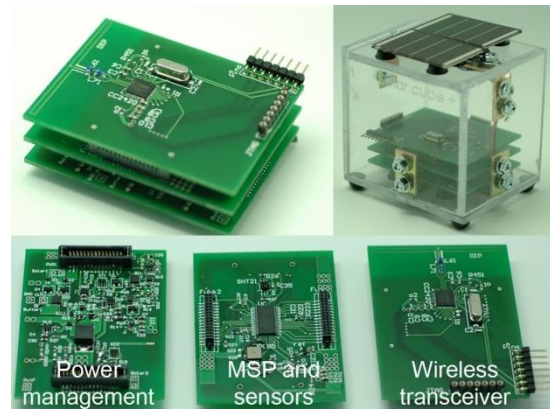
2x CSD25401Q3: <http://focus.ti.com/docs/prod/folders/print/csd25401q3.html>

1x CSD16301Q2: <http://focus.ti.com/docs/prod/folders/print/csd16301q2.html>

1x SN74AUP2G80: <http://focus.ti.com/docs/prod/folders/print/sn74aup2g80.html>

1x REF3312: <http://focus.ti.com/docs/prod/folders/print/ref3312.html>

1x CC2420: <http://focus.ti.com/docs/prod/folders/print/cc2420.html>



Abstract:

The presented system is a power management circuit that operates energy harvesting generators near their maximum power point. With this energy the system can drive different sensors and a wireless transceiver. In order to achieve self-start up and harvesting, a special tracking circuit is developed. Further on, for energy efficient operation the microcontroller is programmed based on an event-driven concept, which allows efficient usage of the low power modes. The device can be used in many different areas, for example to detect environment parameters like temperature and humidity.

1. Introduction and Motivation:

Parameter monitoring using WSN (Wireless Sensor Node) is one of the latest innovations for stepping towards a smart and convenient environment. The opportunity EH (Energy Harvesting) offers to power such sensor systems eases the usage of WSN significantly.

Inspired by the energy harvesting chip design activities on the hosting Chair and based on the experiences Max gathered during his BSc Thesis work in the EH group, the idea of developing such a WSN came up. The intention was basically monitoring and forecasting weather in a comfortable way. The challenge is – since we are not chip designers yet - to construct such a system with off-the shelf devices. We want to show that it is possible nowadays to supply sensors and even a RF transmitter periodically only by the use of environmental energy. Hence, the TI Analog Design Contest was recognized as helpful to get support for our project idea, and to have a platform for presenting it. Max, as the head of the team was responsible for the system design, dimensioning, simulation and experiments. Daniel brings in his experiences on layout and device handling, and Florian takes over programming and supports experiments.

In order to do a weather forecast, three parameters are identified to be monitored: temperature, humidity, pressure. Further on, it requires a minimum of one indoor WSN and one outdoor WSN. Therefore, a WSN is constructed, which comprises a solar panel, a power management unit with extensions for MPPT (Maximum Power Point Tracking) enhanced harvesting, a sensor unit, a radio interface, and a microcontroller based control unit. A base station – not part of the project since already available - can gather all data, display parameter plots, and could even calculate forecasts, e.g. a permanently falling in pressure mean rain could start soon. The indoor monitoring node could be used to implement a smart building control, e.g. closing jalousies in case of too much heat or sun exposure.

2. Theoretical Background

Before starting circuit design, fundamental issues on operation method (MPPT) and feasibility (switch-mode converter) have to be clarified theoretically.

2.1 Maximum Power Point

Maximum power point means that a source is loaded so as to provide maximum power P_{max} . This can be visualized by a simplified source model that has a voltage source with a real source impedance only (Fig. 1(a)). Then, this source provides maximum power in case of impedance matching, i.e. the terminal voltage V_g is just equal to the half of the instantaneous open circuit voltage $V_{g,oc}$. Accordingly, while charging a capacitor the source provides maximum power just in the moment

$$t_{MPP} = R_g C_{in} \ln(2) = \tau_{chg} \ln(2) , \quad (2)$$

i.e. when V_g passes the half of the instantaneous open circuit voltage $V_{g,oc}$ (Fig. 1(b)). Hence, a tracking ratio is $k_{track} = 0.5$.

Now, tracking of this MPP is achieved if the load is controlled such that the source can provide most continuously its maximum power. Related to the load capacitance, this means that an appropriate balance between charging and discharging has to be

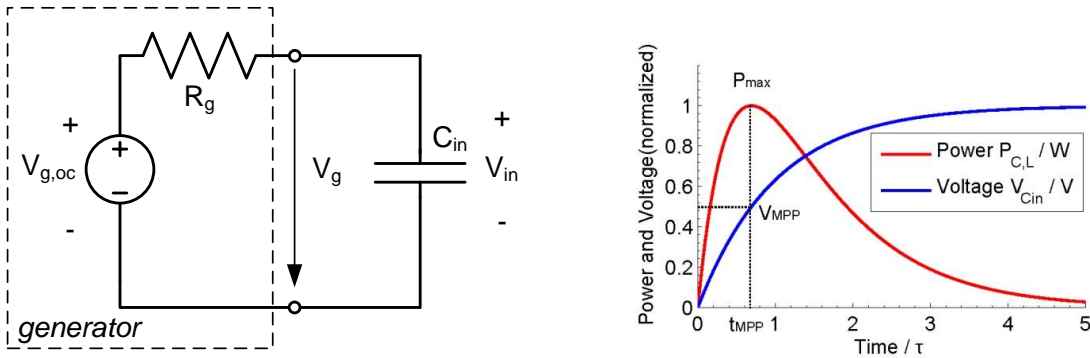
established. This can be realized by allowing a small hysteresis of V_g , i.e. the capacitance C_{in} is charged till V_{stop} , e.g. $V_{stop} = 0.55 V_{g,oc}$, and then discharged to V_{start} , e.g. $V_{start} = 0.45 V_{g,oc}$. By evaluating the integral based on the exponential capacitor charging equations

$$P_{ext} = \frac{1}{2\Delta t} \int_{t_{MPP}-\Delta t}^{t_{MPP}+\Delta t} \frac{V_g^2}{R_g} \left(\exp\left(-\frac{t}{\tau_{chg}}\right) - \exp\left(-\frac{2t}{\tau_{chg}}\right) \right) dt. \quad (3)$$

The extractable power P_{ext} is above 94% of P_{max} as long as the relative hysteresis ($V_{stop}-V_{start}$) is below 10% of the open-circuit voltage $V_{g,oc}$.

Using a real generator instead of such a simplified source model, this tracking ratio (k_{ratio}) between terminal voltage and instantaneous open-circuit voltage differs. In case of the solar panel (Sanyo AM-5412) this ratio is 0.75 instead of 0.5.

Hence, there are two important things: First, such hysteretic MPPT is essential, secondly, a relative small tracking hysteresis can be accepted, and third the tracking ratio has to be programmable.



(a) (b)
Fig. 1: (a) Simplified generator model with a load capacitor, (b) initial capacitor charging curve shows a maximum at t_{MPP} .

2.2 Switch-Mode Voltage Conversion

For establishing the control of C_{in} between V_{start} and V_{stop} , a switch mode converter and a further buffer C_{stg} is needed. Since switching cycles mean losses, and power efficient operation is crucial, a single-step approach is intended.

That is, at V_{stop} the complete energy

$$E_{in} = \frac{1}{2} C_{in} (V_{stop}^2 - V_{start}^2) \quad (4)$$

is transferred into the inductor at a single switch cycle ($I_L(t=0) = 0$)

$$I_{L,peak} = \sqrt{\frac{2E_{in}}{L}}. \quad (5)$$

Hence, by assuming that V_{start} is not much different from V_{stop} the transfer time can be approximated by

$$t_{peak} = L \frac{I_{L,peak}}{V_{stop}}. \quad (6)$$

Solving Eq. (6) with common parameters, e.g. Fig. 2, results in a t_{peak} range of 7-12 μ s. Comparing these values with the given delays in available TI Micropower comparators, these values seem feasible.

3. Implementation

As illustrated in Fig. 2, the WSN comprises (i) power processing chain, (ii) a power management part, (iii) an application part with sensors and radio communication chip, and (iv) a central microcontroller. The power processing chain has three buffers: an input buffer C_{in} , a storage buffer C_{stg} , and an application buffer C_{app} . The power-management is designed so as to allow fast self-startup from a zero-power-level, as well as restarts in case of low buffer voltages, e.g. after a brown-out situations.

3.1 General Power Management Operations

The boost converter between C_{in} and C_{stg} is for the MPPT. Therefore, this boost stage operates in the single-step mode (Theory Section) and is controlled by the LMU (Load Matching Unit). This LMU, in turn, compares the actual voltage on C_{in} with a the optimal tracking voltage (V_{MPP}) of the periodically sampled open-circuit generator voltage ($V_{g,oc}$):

$$V_{MPP} = k_{ratio} V_{g,oc} \quad (7)$$

This voltage provides the open-circuit voltage sampling unit (VSU). Hence, instead its output voltage, this boost stage controls its input voltage, i.e. V_g for realizing the hysteretic MPPT. Since the harvested energy is primarily stored on C_{stg} – which therefore has typically the highest voltage in the system, a buck converter is added supplying a constant voltage V_{Capp} (e.g. 2.2 V) to the applications and microcontroller.

3.2 Power - Management Start-up

The start-up is sectioned in three phases. Starting from a complete uncharged condition, the control signals are set by pull-ups and pull-downs so as to start charging all three buffers in parallel. For reducing excessive leakage through these pull-up and pull-down resistors untypical high values are used, i.e. typically several 100 k Ω . In addition, for avoiding undefined or floating digital signals a Voltage supervisor (VSV, TI TPS3106E16) controls the μ C and the LMU. This initial charging phase I lasts till all three buffers reach approximately 1.5 V, which is set by the VSV.

Then, phase II is entered by activating the LMU. Hence, the boost converter starts operation, which reduces the voltage on C_{in} towards V_{MPP} . Simultaneously, C_{stg} and C_{app} are further charged in parallel until the second trip point of the VSV is passed. There, approximately a V_{Capp} of 2.2 V is reached, and the VSV turns on the microcontroller, too. At this point, phase III starts, and start-up is finished. Hence, also the buck converter can be operated. Thus, the voltage on C_{stg} , will further increase (due to harvesting and boosting), while the μ C controls the buck converter for keeping the output voltage on C_{app} constant.

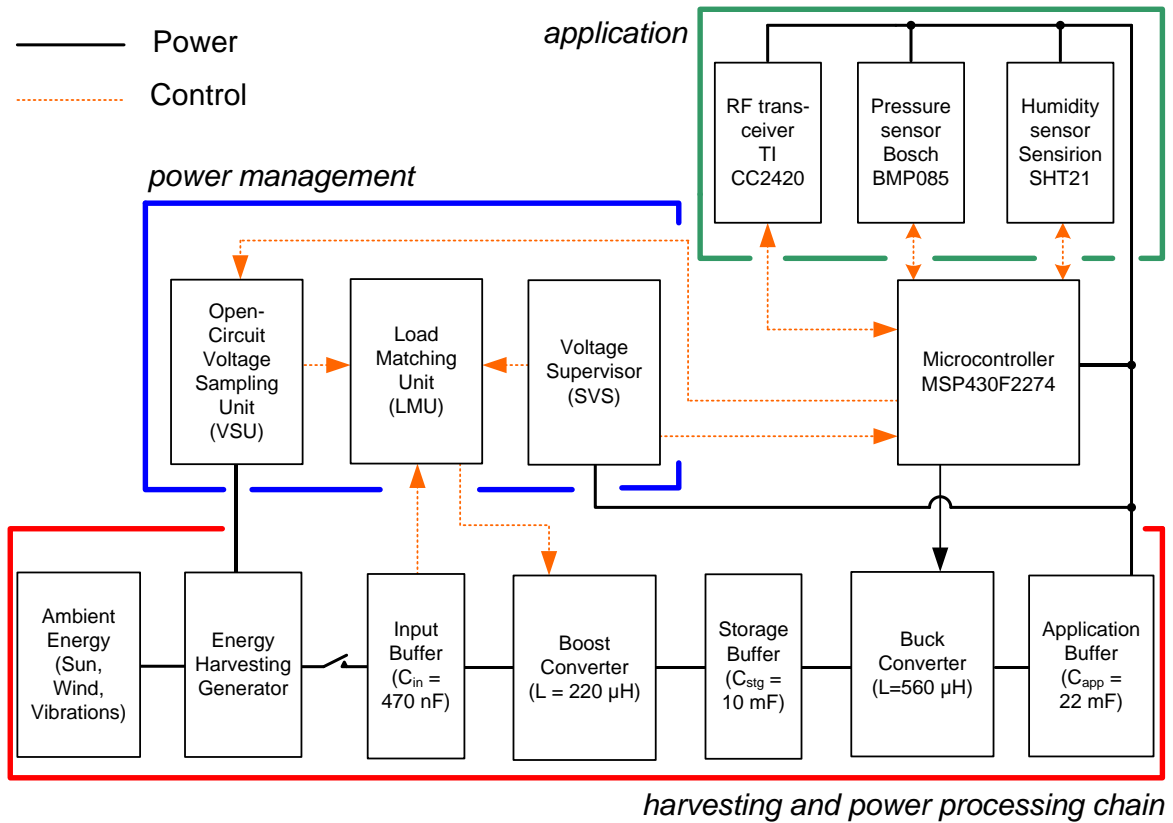


Fig. 2: Overview of the WSN system with all building blocks.

3.3 Voltage Sampling Unit (VSU)

To set V_{MPP} , the open circuit voltage $V_{g,oc}$ is measured periodically. For this measurement, switch M1 disconnects the interface for a short interval (Fig. 3). For avoiding adverse interference during start-up (phase I and II), the VSU has an additional branch for start-up, which is installed by U6, M7, C_{ref2} (Fig. 3). At settled operation (phase III) this branch is permanently turned off.

Phase III: A short sample interval starts with resetting C_{ref1} by turning on switch M6. Thereafter, the hold-capacitor C_{ref1} is ready to sample the actual open circuit voltage. Therefore, the μC turns-off M1 (PMOS M1 TI CSD25401Q3), and C_{ref1} is charged through Schottky diode D3. After t_{sample} , M1 is turned on again, and harvesting can proceed. In parallel, D_{MSP1} frees also the LMU. The tracking ratio k_{track} is programmed with resistor R_{VSU1} and R_{VSU2} . The repetition of such sampling procedures is controlled by the μC and has to be adapted with respect to the dynamic of $V_{g,oc}$.

Phase II: Here, the circuit is still starting-up. One has to note, that the time for phase II ($t_{phase,2}$) is not defined and depends strongly on generator voltage, and its external excitation. Hence, the small C_{ref1} could suffer from excessive discharging (via R_{VSU1} , R_{VSU2} , and D3 leakage) resulting in start-up failure. Therefore, in phase II switch M7 connects a larger capacitor C_{ref2} in parallel to C_{ref1} .

Phase I: Basically all active devices are turned off, i.e. tracking, LMU and VSU are inactive. Switches M6 and M7 are turned off.

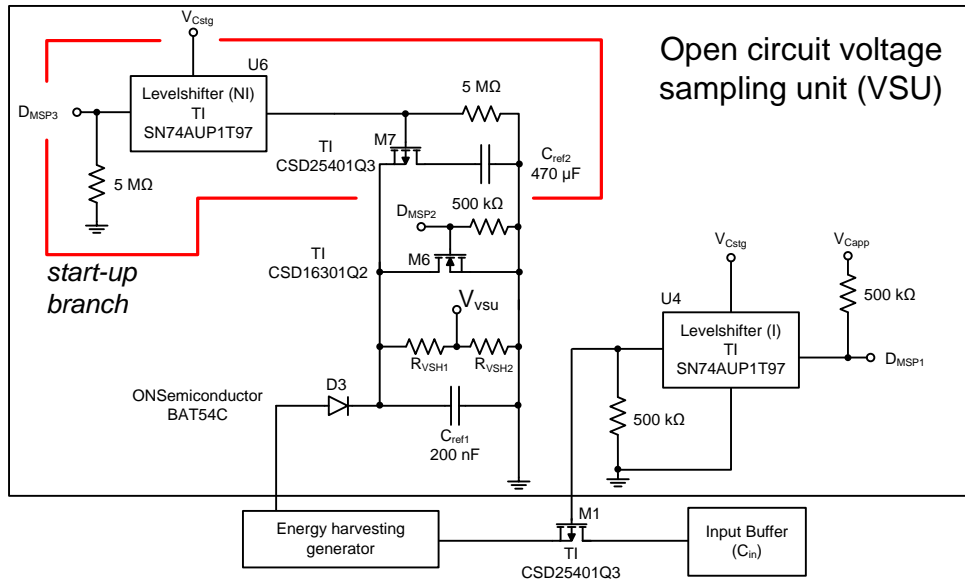


Fig. 3: Voltage sampling unit (VSU) with level shifters.

3.4 Load Matching Unit (LMU)

The LMU controls the low-side switch of the boost converter for realizing MPPT. Basically, there is a Schmitt trigger (ST1) with additional enable signals released by the μC and the VSV (Voltage supervisor). ST1 compares the actual buffer voltage of C_{in} with the tracking ratio of sample voltage V_{MPP} . Hence, the ST1 releases an output signal edge if V_{stop} is reached, and resets its output signal if C_{in} is sufficiently discharged, i.e. the lower trip point (V_{start}) is reached. The hysteresis is set by the resistive feedback network of the ST1. The output signal $D_{boost,on}$ is provided to the low-side switch (NMOS) of the boost converter in case all enable signals are high.

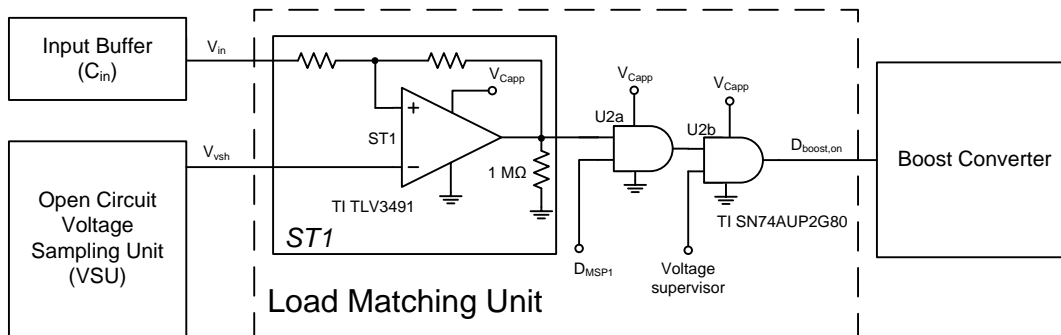


Fig. 4: Load matching unit (LMU) triggers the boost converter.

3.5 Boost Converter Control

The boost converter consists of a low-side switch (NMOS), and a Schottky Diode as a transfer element. The switch is controlled by the LMU so as to achieve MPPT.

3.6 Buck Converter Control

The buck converter comprises a $680 \mu\text{H}$ SMD inductor, a PMOS switch, and a Schottky diode. The PMOS switch is operated with pulse width modulation (PWM) by the microcontroller. For realizing a simple line regulation, a Schmitt trigger (ST2) is dimensioned for a 100 mV hysteresis around the desired output voltage. Hence, this ST2 interrupts the microcontroller in case of under- or over voltage detection.

Correspondingly, the μC starts or stops PWM control for continuous-conduction mode (CCM) operation.

3.7 WSN Application

The application hardware comprises three sensors, and a radio device. And, it uses the μC for the central/complete control. The programming uses an event-handler based approach. That is, an event queue gets filled with events at an interrupt. As long as an event is in the queue, the controller subsequently executes the related event handler function. As soon as the queue is emptied, the controller enters LPM3. Then, the controller wakes not up again before a new interrupt occurred.

This approach has two main advantages. First, it provides a very modular architecture. The extension of functionality, e.g. adding another sensor, used commands or communication protocol, can be inserted just by defining new event handler functions. In addition, the controller enters a low-power mode whenever possible. This reduces power consumption – which is of particular importance since WSN typically have long idle periods.

3.8 Part Selection

The used microcontroller MSP430F2274 is very useful due to its wide supply voltage range (1.8 V - 3.6 V), the diverse sleep mode options help power saving power, and power efficient active modes, e.g. 270 μA at 1 MHz. The low-power ADC is necessary for buffer voltage monitoring, and the timers are important for sleep mode handling. Its various ports allow easy sensor access (I^2C) and radio chip communication (SPI).

Using the CC2420 impressed due to its easy accessing of a μC by SPI, its hardware implemented IEEE 802.15.4 protocol stack – which eases radio communication programming, and its competitive idle and active mode power consumption.

The TI TLV3491, used for all comparators, offers a very low quiescent current loss (0.8 μA), and relatively short delay times, and also a sufficient voltage range.

The built-in voltage reference of the MSP430 consumes relatively large currents. Therefore, the TI REF3312 is added due to its low currents consumption (3.9 μA) and a similar minimum supply voltage than the MSP430.

Since the μC - supplied by C_{app} - also interfaces switches connected to C_{stg} and to the generator, the TI SN74AUP1T97 is inserted for level conversion. Convincing are its flexibility with (non-) inverting ports, and low supply currents (a few μA).

As power switches, the PMOS *TI CSD25401Q3*, and the NMOS *TI CSD1630* are appropriate. Both devices have a low on-resistance paired with small gate-input capacitance. Thus, allowing small conduction losses, and small dynamic drive losses.

4. Simulation

The complete power management system was simulated with PSpice, before building it up on a printed circuit board, in order to verify the functionality of the circuit and to improve the dimensioning of the different components. Instead of using ideal integrated circuits, we implemented all analog TI components with Spice models provided on the TI website. In order to decrease the computing time, the sizes of

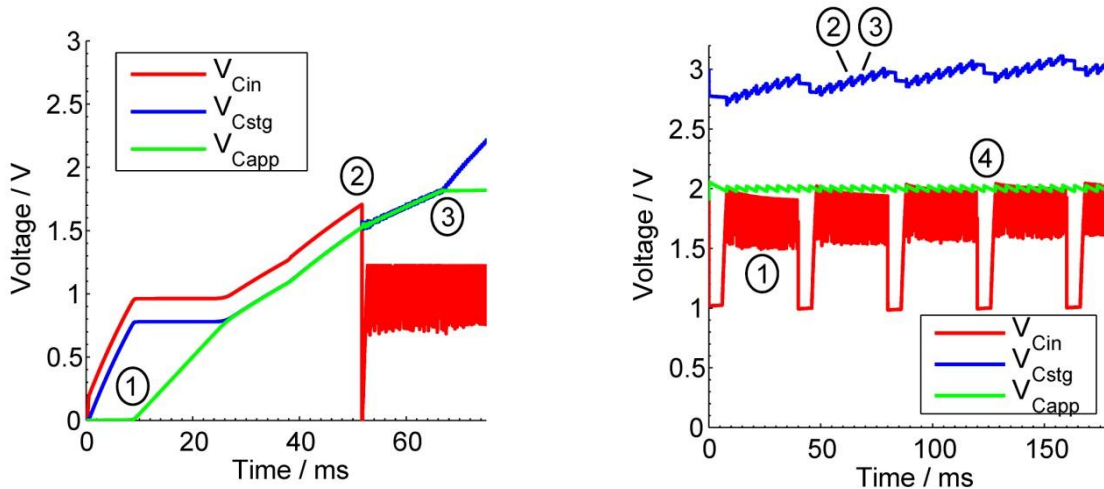
capacitor C_{stg} and C_{app} are reduced. It was taken care of the problem, that the provided simulation models only work correctly in their voltage supply range and might have not the correct functionality during startup.

The simulated startup of the system supplied with a DC generator can be seen in Fig. 5(a). The procedure is in correspondence to phase I, II, and III (Section 3.2).

- At point 1 the voltage at C_{stg} is high enough to open the PMOS of the buck converter between C_{stg} and C_{app} and C_{app} is also loaded.
- At point 2, phase II start. As the boost converter works, the voltage in C_{stg} can reach a higher level than $V_{g,oc}$. Thus it is even possible to startup with low open circuit voltages.
- At point 3, phase III starts, and operates as introduced in Section 3.2.

Fig. 5(b) plots the simulated voltages of all three capacitors during typical operation.

- At point 1 the load matched voltage at C_{in} can be seen. The open circuit voltage was set to 3.5 V. Therefore C_{in} alternates around 1.75 V.
- The ripple between point 2 and point 3 is because C_{stg} is occasionally discharged by the buck converter for energy transfer to the application (C_{app}).
- The open circuit voltage is sampled at point 4, therefore the boost converter is disconnected and the maximum power point tracking is stopped for short time.



(a) Start-up in 3 steps.

(b) Settled operation.

Fig. 5: Transient simulation of the harvesting interface operation.

5. Experimental Results

5.1 Power Management Operation

In order to verify the functionality of the power management the measured voltages at the three buffers during the startup with the solar cell under normal laboratory light are shown in Fig. 6. The results match the expectations from the simulations. The described points in the simulations section are also marked in this measurement.

The measured voltages at C_{stg} and C_{app} during normal operation with a constant load with the solar cells as generator are pictured in Fig. 7. Additionally the signal from

Schmitt-Trigger ST2 is shown. At point 1 the ST2 triggers an interrupt at the MSP430 and energy is transferred from C_{stg} to C_{app} using the buck converter.

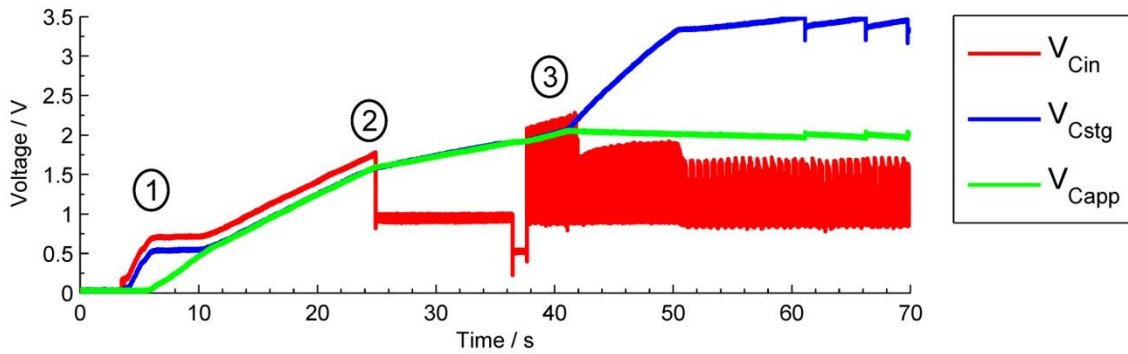


Fig. 6: Plot of measured start-up procedure.

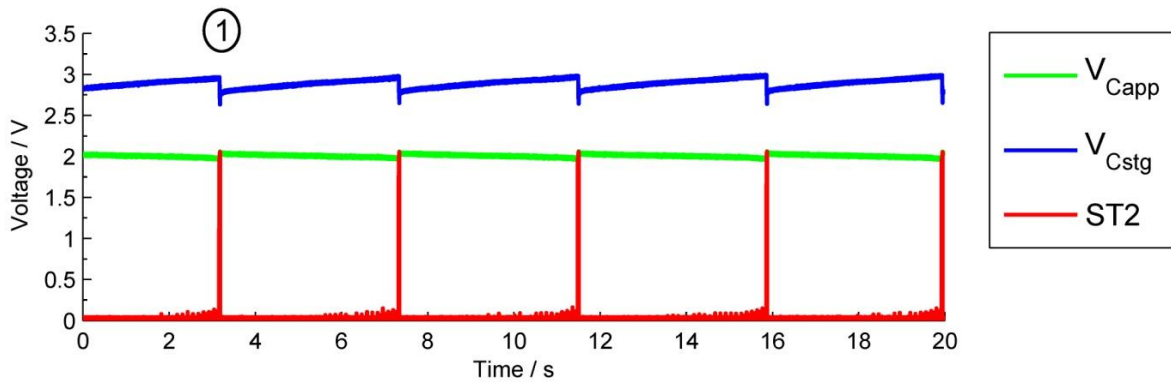


Fig. 7: Plot shows hystereitic control of the application supply voltage V_{Capp} .

Even under heavy load conditions (ca. 20 mA), which appear during RF device operation, the voltage at C_{app} can be regulated to a constant value for a sufficient long time duration. Fig. 8 shows the voltages at C_{stg} and C_{app} if a load of 100 Ω is applied to C_{app} for about 200 ms (points 1). This means the current is about 20 mA.

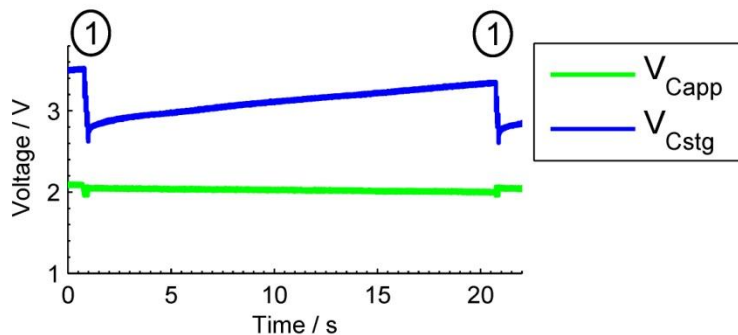


Fig. 8: Load step response if 100 Ω load is connected to the application supply C_{app} .

5.2 Sensors Data Acquisition

The two sensors were tested for about 500 s, measuring one value from one sensor every 30 s. The measurement data were collected walking from 2nd floor of our laboratory building to the basement and then to the outside on a warm and sunny day (blue points) and on a rather cloudy day (green points).

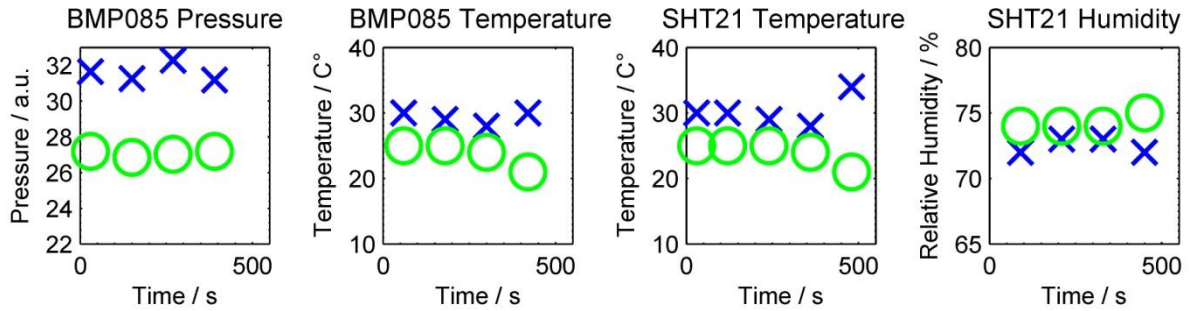


Fig. 9: Gathered sensor data show environmental values during a lab walk around.

6. Conclusion

In sum, we can state that operating a WSN for weather monitoring only powered by a solar panel is possible. The power management unit achieves MPPT and controls an output voltage. In addition, a reliable start-up concept is realized. Data from different sensors are acquired periodically, and even a radio interface can be driven regularly.

During development, particularly managing efficient start-up procedure in conjunction with the VSU was a challenge. Not only for this, had the preceding simulation been very helpful. Altogether, we have a WSN, which includes an energy harvesting interface for efficient start-up, with a hysteretic MMP voltage tracking, and stabilized application supply voltage. The built hardware in conjunction with the event-driven control is a promising platform for starting follow-up projects based on this system.

7. Future Plans

For simplifying the usage of our WSN systems, a direct control via a PC would be admirable. Thus, as a first step, extending our software with a command interpreter is planned. Further on, other generators could be designed to drive this WSN system. This is of particular interest, since the power management tracking unit is actually able to handle AC input voltage, e.g. as provided by electromagnetic generator. A further aspect is the radio communication. Our proprietary protocol stack uses an adapted ZigBee protocol. This avoids time-intensive peering procedures, thus, reduces power consumption significantly. But, adapting the system to standard protocols, e.g. like the SimplciTi protocol, would be a valuable next step. This would also help to widen the field of application, e.g. building or machine monitoring.

8. Acknowledgement

Finally we would like to thank everyone who supported us during the development of our system. At first we want to thank Prof. Dr.-Ing. Yiannos Manoli and the Fritz Huettinger Chair of Microelectronics for giving us the possibility to participate at the TI Analog Design Contest. Especially we want to thank Dominic Maurath for his great technical support around-the-clock and that he always took time for our thoughts. We also want to thank Thorbjörn Jörger for supporting us during the reflow soldering process of our boards and Dirk Buselmeier for the support with the laser cutter.